3rd International Conference on New Developments in Soil Mechanics and Geotechnical Engineering,
28-30 June 2012, Near East University, Nicosia, North Cyprus

Numerical back-analysis of a deep excavation consisting of multipropped retaining wall

Mohamed Nabil Houhou
Department of Civil Engineering, Mohamed Khider University, Biskra, Algeria, houhounabil@yahoo.fr

Fabrice Emeriault
Grenoble-INP,UJF-Grenoble 1, CNRS UMR 5521, 3SR Lab, Grenoble F-38041, France

Richard Kastner
LGCIE, INSA, Lyon, FRANCE

KEYWORDS: Deep excavation, numerical modelling, retaining wall, soil-structure interaction.

ABSTRACT: The construction of a deep excavation in an urban environment behind flexible retaining structures requires that the generated movements are limited to prevent damage to adjacent structures and works. In this context, this article examines the three-dimensional numerical modelling with a finite difference code of a monitored deep excavation consisting of a diaphragm wall supported by several rows of steel struts. The Saint-Agne station is located on the Toulouse (France) subway line B and is built in an overconsolidated molassic geological context. The set of measurements obtained with different monitoring devices have been confronted with the numerical back-analysis (2D and 3D) using a finite difference code in which the dewatering is taken into account through an uncoupled flow-mechanical calculation. The obtained results are in good agreement with the different measured data. The model also gives an insight on the 3D behaviour of the excavation and its impact on the existing brick building.

1 INTRODUCTION

The urban development often requires the use of the underground space. Deep excavations associated with the realization of basements of buildings, underground parking or subways are generally maintained by retaining walls with multiple supports (props or anchors). Soil excavation causes deformations, both horizontal and vertical, of the surrounding grounds. These deformations, induced by the excavation and the underground flow generated by the dewatering at the bottom of the excavation can cause damages to the neighbouring structures and must be carefully controlled during the execution of the works. The induced deformations of buildings in the vicinity of the retaining wall are crucial because they dictate the level of damage which may occur (Mair et al. 1996).

The traditional methods of calculation based on limit equilibrium or subgrade reaction method have been proved to be inaccurate (Vanoudheusden et al. 2005, Descœudres & Pellet 1991). Numerical methods such as Finite Element Method or Finite Difference Method (either in 2D or 3D) are now considered as standard methods to analyze this type of problem. Despite the numerous developments of specific numerical codes and their encouraging results, discrepancies are still observed during comparison of numerical simulation of such structures with monitored sites. The observed differences can be partly explained on the one hand by the difficulty of accurately accounting for the real conditions of construction of the works and on the other hand by difficulties

in estimating the evolution of lateral stresses in the soil (due to the anisotropic small-strain non linear behavior of the soil).

In this context, this article examines the three-dimensional numerical back-analysis of a monitored deep excavation consisting of a diaphragm wall supported by several rows of steel struts. The Saint-Agne station is located on the Toulouse (France) subway line B. The object of this analysis is to estimate the behavior of the excavation in terms of displacements of diaphragm walls and the development of load in struts, as well as the impact of the excavation on the existing buildings (horizontal and vertical deformations) and to shed some light on the three-dimensional nature of the movements induced by the excavation.

The explicit finite differences numerical code FLAC^{3D} (Itasca 2006) is used to model the excavation, its different constituents and the various phases of realization. The dewatering is taken into account through an uncoupled flow-mechanical calculation. The results of this 3D model are confronted with those of the campaign in-situ measurements. The pertinence of the 3D model is also judged by comparison with the 2D plane strain model, implemented in the FLAC^{2D} code.

2 PROJECT DESCRIPTION AND INSTRUMENTATION

Saint-Agne station is a 55.2 m x 17.15 m rectangular box with a 20.65 m long and 1 m thick diaphragm wall (Figure 1). The 17.2 m deep excavation requires the use of three levels of temporary steel struts 0.61 or 0.66 m in diameter and 10.3 or 12.7 mm thick (Figure 2). Table 1 summarizes the different excavation phases and schedule.

Two fully equipped monitoring "sections" have been installed on the Saint-Agne excavation site (Figure 3): Section 2 corresponds to "Greenfield" conditions whereas Section 1 includes a 9m x 27m old brick building perpendicular to the excavation with a minimum distance to the diaphragm wall equal to 2 m. Each section includes one inclinometer in the diaphragm wall, 4 vibrating wire strain gauges installed at mid-span on each of the three strut levels (with automatic data acquisition) and precise levelling. Horizontal extension of the brick building is measured on several intervals with an invar thread.

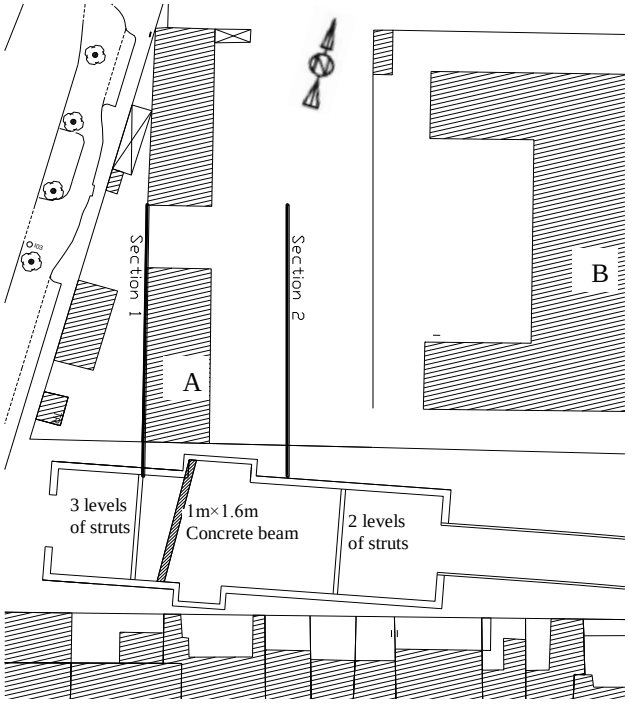

Figure 1. Global view of the site

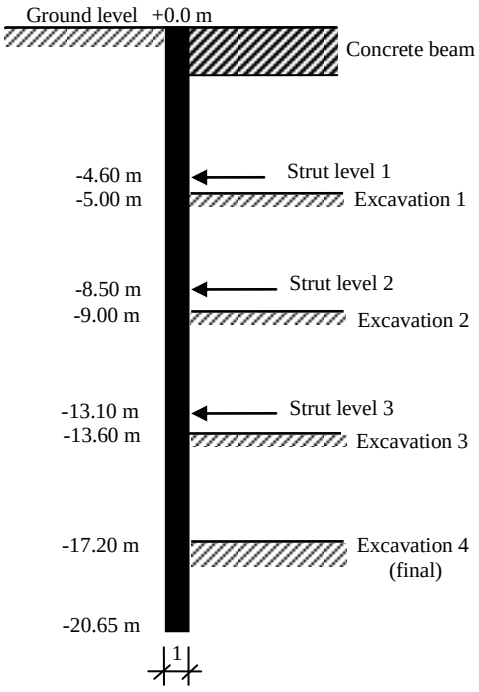

Figure 2. Cross-section of the diaphragm wall

3 GEOLOGICAL CONDITIONS

The regional geological substratum is constituted by molassic formations dating from the Tertiary. These grounds have been overtopped by a minimum of 200 meters of Stampien and Miocene which have been eroded before the deposition of the quaternary alluviums. In fact, the Toulouse molasses exhibit a very high overconsolidated behavior with in particular a high value of the at rest earth pressure coefficient K_0.

The encountered geology is homogeneous on the whole layout of the line B project. The tunnels run through the Toulouse molasses (hard sandy clay with pockets and lenses of very dense sand). Geotechnical investigations have shown that in these formations, the geotechnical characteristics are homogeneous (the unit weight $\gamma = 22$ kN/m^3 ; the undrained cohesive strength $c_u = 300$ kPa ; the cohesive strength $c' = 30$ kPa ; the angle of internal friction $\varphi' = 32°$). In the case of Saint-Agne station, the molasses are found between 1.2 and 2.0 m below ground level and the water table is approximately 2 m below the ground level.

High pressure K_0 oedometer tests (Serratrice 2005) have also shown that the overconsolidated molasses is subject in-situ to very high horizontal initial stress (K_0 is estimated equal to 1.6).

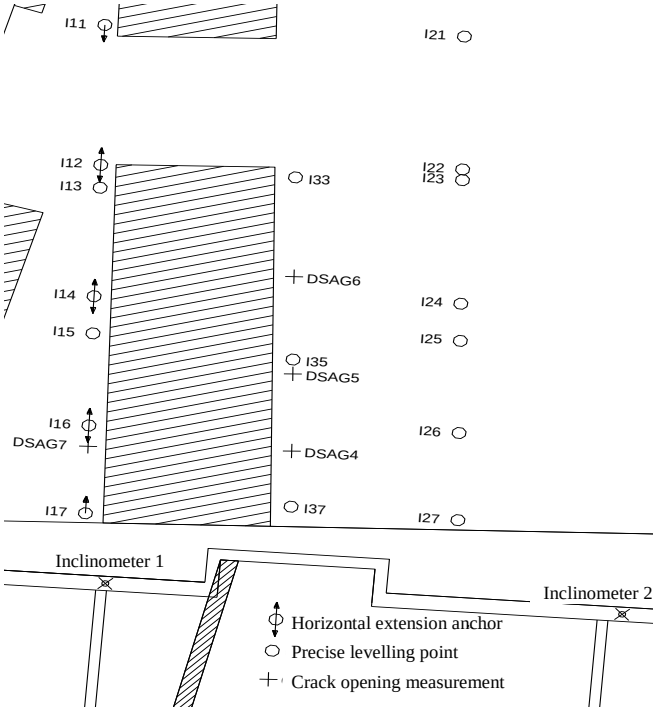

Figure 3: Location of the instrumentation

stage	activity	Date	Level (m)
1	preexcavation	07/04-02/06/03	-1.9
	Partial concrete slabs and beams (west side)		+0.0
2	Excavation 1	05/06-18/06/03	-5.0
	Middle slab	19/06-07/07/03	-5.0
	Cover slab (east side)		+0.0
	strut 1	23/06-02/07/03	-4.6
3	Excavation 2	30/06-11/07/03	-9.0
	strut 2	01/09-12/09/03	-8.5
4	Excavation 3	12/09-01/10/03	-13.6
	strut 3	13/10-21/10/03	-13.1
5	Excavation 4	30/10-28/11/03	-17.2
6	concrete slab	3/12-03/02/04	-16.85
	Removing strut 3	23/01-03/02/04	-13.1

Tableau 1. Excavation phases and schedule

4 THREE-DIMENSIONAL NUMERICAL MODELING

The finite difference formulation was designed to simulate the various phases of excavation such as dewatering, soil excavation process, strut installation, slab concreting, …. To limit boundary effects on the behavior of the ground near the walls, the mesh extends laterally 50 m away from the walls and vertically 35 m below ground level (Figure 4). Standard boundary conditions have been considered. These boundaries are supposed to be impervious. The level of the water table is maintained constant 2 m below ground level outside the walls. The level inside is supposed to be horizontal and modified at each stage of dewatering.

The passive strut is normally subjected to axial force, therefore bar elements have been used to represent struts. The walls and concrete slabs were meshed using parallelepipedic elements. The walls, struts, and concrete slabs are assumed to behave as a linear-elastic material. However, the behavior of the soil is modeled with a linear elastic – perfectly plastic constitutive law using the Mohr-Coulomb failure criterion. The contact between the diaphragm wall and the soil is considered adherent. A posteriori, it has been verified that this assumption does not induce any development of plastic zones in the soil elements in contact with the wall.

The existing buildings on the south side were simulated by a 15 kPa pressure uniformly distributed. However, building A (cf. Figure 1) is modeled by volume elements linked to the mesh by an interface defined by a normal and shear stiffness. The relative shear displacements are controlled by a Mohr-Coulomb friction law. The system of shallow foundations was not represented explicitly. To account for the presence of water in the calculations, an uncoupled flow-mechanical calculation process has been used to model the effect of successive lowering of the water table (the effect of the deformations on the pore pressures has however been neglected).

Given all the tests carried out and the dispersion of values, a linear variation of Young's modulus E of the soil with depth z is proposed: $E\ (MPa) = E_0 + \beta.z = 66 + 9.9\ z\ (m)$.

This linear variation is also based on the numerical back-analysis of the excavation of a 8.0 m in diameter tunnel in the vicinity of the project and of the Jeanne d'Arc station instrumented in a similar way (Houhou et al. 2010).

5 BEHAVIOR OF THE DIAPHRAGM WALL

The diaphragm wall itself is instrumented by two inclinometers while the different struts are equipped with vibrating wire strain gauges. Figure 5 shows that the maximum horizontal displacements (δ_{hm}) present a strong variation along the wall, which reflects well the corner stiffening effects already mentioned by Houhou et al. (2010) and Finno et al. (2007). The effect of geometrical singularity of the excavation is also very clear. At the final stage of excavation (step 6), the displacements predicted by the 2D analysis are relatively overestimated throughout the wall. This suggests that an effect of corners persists and that the plane strain conditions do not prevail even in the central sections of the long side of the wall. The ratio δ_{hm} /H is close to 0.05 %. This value corresponds to low values over the range given by Long (2001) and Leung (2007). This can be attributed to the use of relatively rigid diaphragm walls and overconsolidation of the soil mass.

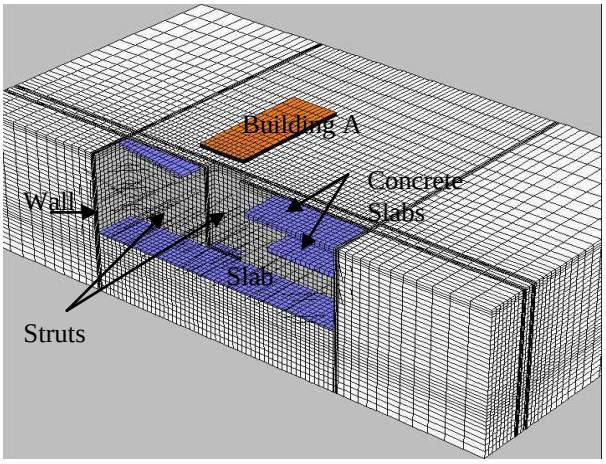

Figure 4. Half mesh used.

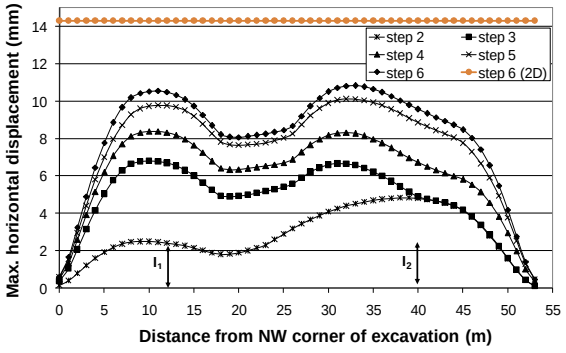

Figure 5. Distribution of the maximal horizontal movements along the wall.

Figures 6 and 7 present a confrontation of calculated horizontal wall displacements with those measured by the inclinometers I_1 and I_2. A lack of grouting in the upper part of the inclinometer casings lead to discard all the values measured for the first 3 m. Nevertheless, it appears that the movements obtained are very similar in shape and amplitude, the displacements being slightly greater in the case of Inclinometer 1 (at the final stage δ_{hm} is close to 11.2 mm instead of 10.2 mm for Inclinometer 2). Because the final embedment length of the wall is rather small (3.45 m), a global rotational movement is observed in the lower part of the wall. In the upper part, a partial concrete slab (0.4 m thick) and a concrete beam (1.6 m high and 1 m thick) induce in the vicinity of Inclinometer 1 an increase of stiffness (cf. Figure 1). This explains that the behavior of the top part of wall is mainly rotational whereas for the Inclinometer 2, the observed movement corresponds to a deflection towards the centre of the excavation.

The confrontation of calculated and measured displacements shows that the computation results tend to overestimate slightly the measurements in the calculation steps 2, 3 and 4. However, after the 5th and 6th step, the computation results and measurements are very similar, both for the shape of the curves and the orders of magnitude of displacements. Globally we observe that the shapes of the deflection are correct, in particular with regard to the point positions of maximum deflection.

The strut loads are measured through monitoring of 2 different cross sections of struts, located close to the inclinometers (Figure 3). For Section 1, the strut loads are monitored in the three levels of steel struts denoted 1-1 (upper), 2-1 (middle) and 3-1 (bottom). It is reminded that a 1 m x 1.6 m concrete beam is constructed across the excavation at the top of the diaphragm wall and that the load carried by this beam is not measured. For Section 2, two levels of struts are used (denoted 2-2 and 3-2), a partial concrete slab is constructed at the top of the wall at the end of Phase 2.

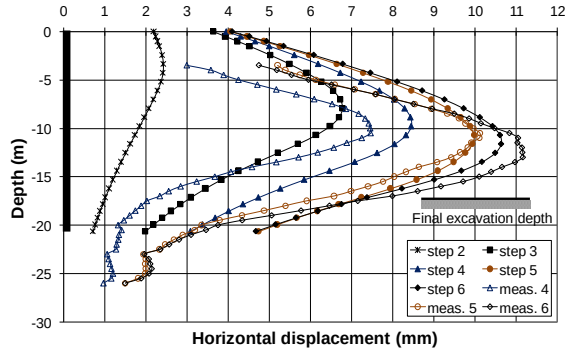

Figure 6. comparison of simulation and measurements of the inclinometer I_1

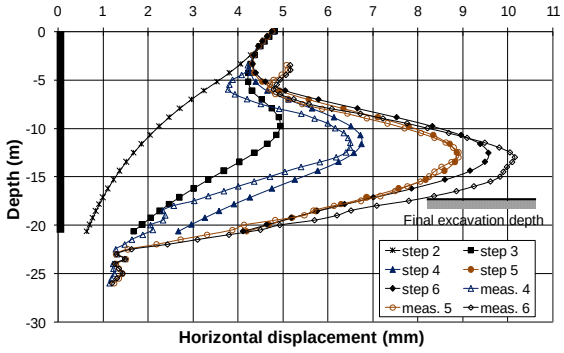

Figure 7. comparison of simulation and measurements of the inclinometer I_2

Figure 8 summarizes the measured and calculated strut loads at the end of Phases 3, 4 and 5. It is noted that the different excavation phases lead to an increase in struts load. Comparing the calculated axial loads with the measured ones, it appears that the results are quite exploitable and very satisfactory for the upper and middle struts. The loads measured in these struts are on average close to the calculated values, with uncertainties closely related to the measuring mode and the temperature variation. Regarding the bottom struts, the calculated load in the strut 3-1 is relatively comparable to measurements. However, the calculated effort in the strut 3-2 is about 2 times larger than the measured value. The difference noted in the strut 3-2 is probably due to measurement error. Because it was noted during the instrumentation that this strut was badly stalled and that it is only after a while that it begins to be compressed (Bonnet et al. 2005).

The 2D calculation revealed that loads are always larger than those predicted by the 3D model in a variable ratio with the phase and position of the struts. For the final excavation phase, a difference of 18%, 38% and 50% was observed for the upper, middle and bottom struts respectively.

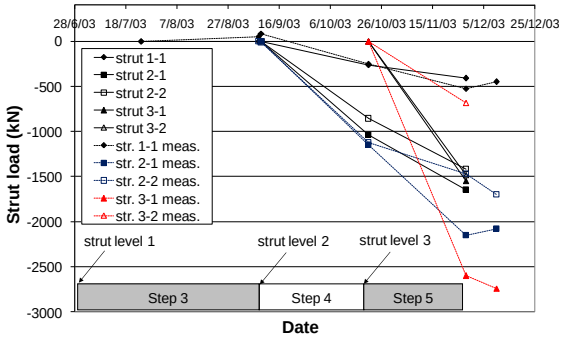

Figure 8. Comparison of calculated and measured axial forces in struts.

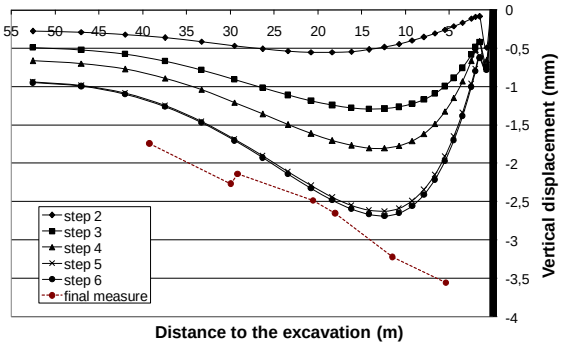

Figure 9. Grennfield calculated settlement trough

6 SOIL-STRUCTURE INTERACTION

The soil-structure interaction is evaluated through the monotoring of a one- storey brick building (Section 1- see Figure 1). The analysis first concentrates on surface settlements along the West facade of the building (points I11 to I17, cf. Figure 3) and on greenfield settlements (points I21 to I27, Section 2) and focuses then on horizontal deformations of this building.

The numerical calculation clearly shows a settlement profile of concave shape, with increasing amplitude with the depth of excavation (Figures 9 and 10). This shape is consistent with the deep inward profiles of the wall deflection observed in figures 6 and 7.

At the end of the excavation phases, the maximum settlement δ_{vm} reached below the brick building is about 3.1 mm (against 2.7 mm in "Greenfield" conditions) and is obtained at 13.5 m from the top of the wall. The maximum vertical displacement is not influenced by the presence of the light brick building, the building (and its horizontal stiffness) only affecting the form of the settlement trough. Moreover, the global stiffness of the diaphragm wall seems to be equivalent in the two cases even though:

- for Section 1, the large concrete beam reduces the possible deflection of the wall
- for Section 2, the irregular shape of the diaphragm wall increases its stiffness.

The amplitude of the surface settlement is lower than that of the horizontal displacements of the wall. The ratio δ_{vm}/δ_{hm} is close to 0.3 %. This low ratio can be partly explained by the high shear strength of the molasses and the high value of K_0.

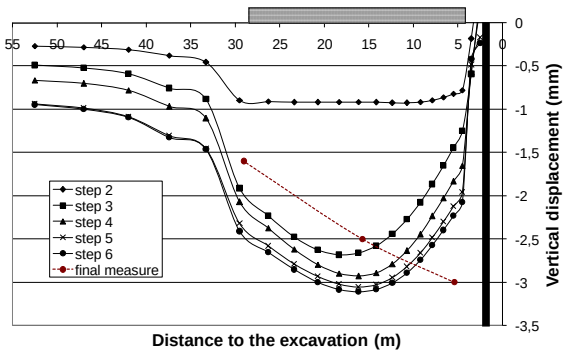

Figure 10. Settlement trough calculated on the west side of the instrumented building.

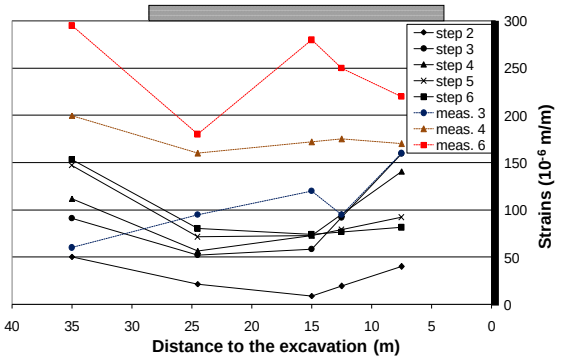

Figure 11. Comparison of calculated and measured horizontal extension.

In terms of order of magnitude of maximum settlements at the end of works, calculated and measured settlements are very comparable. It is noteworthy that unlike the measures for the western façade of the building, the numerical analysis does not provide the fast decrease measured in the settlements of the north side of the building (the farthest from the top of the wall). However, in greenfield conditions numerical calculation predicts a relatively significant decrease in the same manner as the measurements.

Horizontal extensions measurements on the West façade of the brick building A, which can highlight the evolution of the distance between two points (I12 and I14, I14 and I16, I16 and I17 then I14 and I17, cf. Figure 3) over time, are carried through an invar thread convergencemeter. The horizontal extension ε_h between two points is calculated analogously to the real measurement as the difference between the horizontal displacements of these two points divided by the corresponding horizontal distance. It is represented midway between the two points.

Figure 11 shows that an extension is developed along the facade from the first phase of work. This extension does not cease to evolve with the depth of excavation in the zone furthest away from the wall. According to figure 11, we observe overall that the calculated horizontal extensions seem underestimated compared to measurements (by a factor of approximately 0.5). The total increase of calculated distance between points I11 and I17 is about 3.4 mm at the end of stage 6 against an measured increase of 8.6 mm. At the same time, Figure 6 shows that the deflection of the top of the wall is close to 3.3 mm. The difference can be partly explained by measurements errors of horizontal extension. It could also be assumed that there is an approximately 5 mm overall horizontal displacement of the wall itself. Unfortunately, measurements of the horizontal displacements of the wall by total station are not available to check this assumption.

7 CONCLUSIONS

The set of experimental results, obtained during the excavation of the 17.2 m deep Saint-Agne subway station, provided an opportunity to validate a numerical model with a finite difference code. The three-dimensional numerical back-analysis of this excavation was carried out using the finite difference code FLAC^{3D} (the 2D analysis in plane strain is inaccurate due to the effect of the corners and of the irregular shape of the diaphragm wall). It includes the geometrical and mechanical characteristics of the various constituents (soil, diaphragm wall, steel struts, concrete slabs) as well as the phases of excavation and dewatering.

The obtained displacements and settlements remain rather limited (compared to the values given in the literature). Possible explanations of these results include the improvement of the construction techniques, the number of struts (and their characteristics) used in this particular case study but also the good mechanical properties of the Toulouse molasses.

The results obtained are overall satisfactory: the transitional and final deflections of the wall are correctly represented, the profiles of maximum displacement of the wall along to the long side are well described (in particular reduction in displacement due to the corners of the wall), the settlements along a transverse profile as well as the effects on the existing building (settlement and horizontal deformation).

Some points still remain to be improved, in particular:

- The axial loads in the struts are, in particular during the final phase, relatively underestimated. This relative reduction of efforts can be however eliminated by envisaging a more complete modeling of the struts, which allows in particular to represent the nonlinear behavior of these structural elements.
- Similarly, the use of an elastoplastic model with Mohr-Coulomb criterion, which is justified in the first approach by the highly overconsolidated character of the molasse and the essentially elastic behavior of the massif, remains a very strong assumption. It would be advisable to take into account a more sophisticated model for a fine analysis of the results.

REFERENCES

Bonnet, E. T., Emeriault, F. & Kastner, R. (2005). Métro de Toulouse-Ligne B : Auscultaion-Instrumentation sur station, Lot 5-Station Saint Agne, Rapport No. 6.

Descœudres, F. & Pellet, F. (1991). Comportement de l'écran de soutènement d'une tranchée expérimentale étroite. Revue Française de Géotechnique, No. 55, pp. 5-15.

Finno, R. J., Blackburn, J. T. & Roboski, J. F. (2007). Three-dimensional effects for supported excavations in clay. J. Geotech. Geoenviron. Eng., vol. 133, No. 1, pp. 30-36.

Houhou, M. N., Emeriault, F., Kastner, R. & Benmebarek, S. (2010). Rétro-analyse tridimensionnelle d'une excavation profonde multi-supportée instrumentée. Revue européenne de genie civil, Vol. 14, No. 1

Itasca Consulting Group, Inc. (2006). FLAC^{3D} Version 3.1 User's Guide, Minneapolis, Minnesota.

Leung, H. & Ng, C. (2007). Wall and ground movements associated with deep excavations supported by cast in situ wall in mixed ground conditions. J. Geotech. Geoenviron. Eng., vol. 133, No. 2, pp. 129-143.

Long, M., (2001). Database for retaining wall and ground movements due to deep excavations. J. Geotech. Geoenviron. Eng., vol. 127, No. 3, pp. 203-224.

Mair, R. J., Taylor, R. N. & Burland, J. B. (1996). Prediction of ground mouvements and assesment of risk of building damage due to bored tunnelling. Proceeding Geotechnical Aspect of Underground Construction in Soft Ground. Mair and Taylor (eds), Balkema, Rotterdam.

Serratrice, J. F. (2005). Métro de Toulouse – Ligne B : Essais de laboratoire, Rapport No. 22546-01, CETE d'Aix.

Vanoudheusden, E., Emeriault, F. & Kastner R. (2005). Comportement d'une paroi moulée en site urbain. XVIème Congrès International de Géotechnique, pp. 1141-1144. Osaka (Japon).